Polarimetric Properties of Indoor MIMO Channels for Different Floor Levels in a Residential House

S. R. Kshetri[1], E. Tanghe[1], D. P. Gaillot[2], M. Liénard[2], L. Martens[1] W. Joseph[1],
[1]iMinds-INTEC/WiCa, Ghent University, Ghent, Belgium, sunil.kshetri@intec.ugent.be
[2]IEMN/TELICE, University of Lille 1, Lille, France, davy.gaillot@univ-lille1.fr

***Abstract*—This paper analyzes polarimetric characteristics of power delay profiles (PDPs), cross polarization discrimination (XPD), and received power of specular and diffuse multipath components of MIMO radio channels at 2.45 GHz. Measurements were done in a residential house at two floors levels: "same floor" and "cross floor". Variations of 5 to 15 dB in PDPs between co- and cross-polar links were found in the same floor level; however these changes decrease as links move from line-of-sight to non-line-of-sight. XPDs of the radio waves were found to be higher for the cross floor configuration, about 5 dB in horizontally and 7 dB in vertically polarized waves. Also, diffuse components of the radio channels were less affected in cross-polar subchannels compared to that of specular components in the same floor level. The results demonstrate the contribution of diffuse components to the total channel power is higher than previously presented studies for indoor environments.**

***Index Terms*—channel sounding, multipath estimation, specular multipath, dense multipath, Multiple-Input Multiple-Output (MIMO), residential environment, polarization, path loss**

I. Introduction

Indoor propagation measurements, in residential houses, in office buildings or in industrial production halls, are the first and crucial steps towards understanding and characterizing radio wave propagation mechanisms. They provide wireless system designers vital information about wireless radio channels, for example coverage prediction models for wireless networks, in those environments. Several measurement campaigns have been conducted, e.g., IEEE802.11 [1], and ZigBee [2]. The former wireless standard is popular in residential and office environments, whilst the later is known for home automation and industry applications. Moreover, due to ever growing fame of Internet of Things (IoTs) applications and their influence to enhance human productivity as well as living standards, indoor propagation measurements and modeling are an active research field.

Thus, the goal of this paper is to analyze polarimetric characteristics of indoor multiple-input multiple-output (MIMO) wireless channels across different floor levels in a residential house from double-directional measurements at 2.51 GHz carrier frequency.

Few related works have been published concerning the polarization properties of MIMO radio channels. The behaviors of horizontally and vertically polarized electric fields were discussed in [3]. Propagation measurements at 4.5 GHz in an urban environment were performed in [4]. Angular properties of both specular multipath components (SMC) and diffuse multipath components (DMC) of wireless radio channels were reported in [5], whilst [6] discussed about both angular and shadowing characteristic of indoor radio channels in a large university building. More recent studies on polarization properties of indoor MIMO channels can be found in [7] for a large industrial hall.

[8] introduced a first model of DMC in the time delay domain, underscoring the fact that inclusion of DMC in channel sounding date would considerably contribute to radio channel capacity in MIMO links. Later, it drew significant attentions in propagation and measurement research communities, and many supporting results, ie., indoor radio channels compose of both SMC and DMC, have been published for modeling indoor radio channel [6] [9] [10] [11]. Less work, however, has been done to investigate the polarization behaviors of indoor radio channels. Therefore, the main contribution of our paper is to minimize this gap by investigating polarimetric characteristics of indoor MIMO channels from real measurement data.

II. Measurement Scenarios and Procedures

A. Scenarios

The propagation measurement campaign was executed in a residential house located in a rural area (Nevele, west of the city of Ghent) in Belgium. The house has two equal sized floors, approximately 10 m (width) and 20 m (length). The floor plan of the ground floor is shown in Fig. 1. The ground floor consists of a large living room, two dining rooms, a kitchen and an office room. The first floor, not shown here because of space limitation, comprises of four bed rooms, two shower rooms, and one dressing room.

Table I lists the measurement scenarios, including transmitter (Tx) and receiver (Rx) links. Sixteen Tx and Rx links were measured inside the house and grouped into two scenarios: 1) same floor and 2) cross floor. In the same floor case, both the Tx and Rx were placed on the ground floor, and the Tx was fixed at the lower-left corner, indicated by Tx1 (in red) in Fig. 1, while the Rx was moved to eight locations

TABLE I: SUMMARY OF MEASUREMENT SCENARIOS

Links	Situations	Floor label
Tx1Rx1, Tx1Rx2	LOS	Same
Tx1Rx3, Tx1Rx4, ..., Tx1Rx8	NLOS	Same
Tx2Rx1, Tx2Rx2, ..., Tx2Rx8	NLOS	Cross

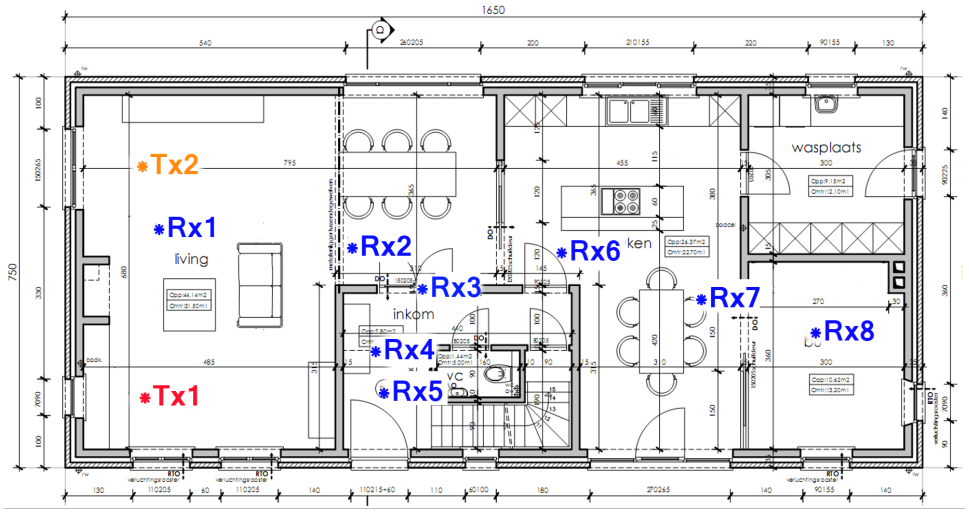

Fig. 1: Floor plan indicating Tx-Rx locations

pointed out by Rx1,...,Rx8 (in blue) across different rooms are shown in Fig. 1. These links represent the first eight TxRx links and encompass both line-of-sight (LOS) and non-line-of-sight (NLOS) conditions also listed in Table I. Similarly, in the cross floor case, the remaining eight links were measured; the Tx was located at a bed room of the first floor, and the Rx was moved to the same eight locations on the ground floor indicated in Fig. 1. For the illustration purposes, the location of the Tx, for the cross floor case, is indicated by Tx2 (orange color) in the same Fig. 1.

B. Procedures

A Vector Network Analyzer (VNA) of Rohde & Schwarz (ZNB20) was used to measure the radio channel, utilizing a frequency domain MIMO channel sounder that was operated at 2.51 GHz center frequency with 80 MHz transmission bandwidth. The bandwidth was sampled uniformly at $M_f = 200$ frequency points. Proper calibration of feeder cables for the transmitting antenna and the receiving antenna was done in the VNA to avoid contaminating the measured data.

A virtual antenna array, consisting of two planar horizontal Uniform Circular Arrays (UCAs) of eight antenna each stacked vertically, was created by an automated positioning system at Tx and Rx link ends. The complete virtual array composes of $M_T = 16$ $(M_R = 16)$ antenna elements. For each position of Tx and Rx link, the VNA took one sweep of the frequency range. Dual-polarized patch antennas were used to access the horizontal (H) and vertical (V) polarization state of the radio waves at Tx and Rx separately through a software controlled switch.

III. Polarimetric Channel Estimator

A. Approach

To detect the number of multipath components and to estimate the radio channel parameters, we applied the extended RiMAX algorithm that includes Effective Aperture Distribution Function (EADF) detailed in [12]. RiMAX algorithm is a multidimensional high resolution channel estimator [8] that considers the radio channels consist of two components: first, SMCs, representing the superposition of highly concentrated multipaths components, and second, DMCs, resulting from the diffuse or random scattering of the radio waves that are prevalent in indoor environments.

B. SMC and DMC Estimation

Polarimetric response vectors $\boldsymbol{h}_{XY} \in \mathbb{C}^{M_R M_T M_f \times 1}$ can be written as the sum of an SMC part $\boldsymbol{s}_{XY}$, a DMC part $\boldsymbol{d}_{XY}$, and a measurement noise part $\boldsymbol{n}_{XY}$:

$$\boldsymbol{h}_{XY} = \boldsymbol{s}_{XY}\left(\boldsymbol{\theta}_{s,XY}\right) + \boldsymbol{d}_{XY}\left(\boldsymbol{\theta}_{d,XY}\right) + \boldsymbol{n}_{XY}\left(\sigma^2_{XY}\right) \quad (1)$$

The subscripts X and Y, either can be horizontal (H) or vertical (V), denote transmitting and receiving antenna polarization respectively, and $\boldsymbol{h}_{XY}$ is modeled as a multivariate circularly symmetric complex Gaussian distribution [8]:

$$\boldsymbol{h}_{XY} \sim \mathcal{N}_c\Big(\boldsymbol{s}_{XY}\left(\boldsymbol{\theta}_{s,XY}\right), \boldsymbol{R}_{XY}\left(\boldsymbol{\theta}_{d,XY}, \sigma^2_{XY}\right)\Big). \quad (2)$$

SMC parameter vector $\boldsymbol{\theta}_{s,XY}$, angles of arrival (AOAs), angles of departure (AODs) and times of arrival (ToAs), correspond to the geometrical parameters and are identical across all four polarimetric subchannels XY; however, the complex amplitudes $\boldsymbol{\gamma}_{XY}$ of the SMC parameter vectors differ between different polarization subchannels due to the polarization-dependency of radio waves interactions.

The DMC covariance matrix $\boldsymbol{R}_{XY}$ in (2) assumes following Kronecker products structure [8]:

$$\begin{aligned}&\boldsymbol{R}_{XY}\left(\boldsymbol{\theta}_{d,XY}, \sigma^2_{XY}\right)\\ &= \boldsymbol{R}_{d,XY}\left(\boldsymbol{\theta}_{d,XY}\right) + \sigma^2_{XY}\boldsymbol{I}_M\\ &= \boldsymbol{I}_{M_R} \otimes \boldsymbol{I}_{M_T} \otimes \boldsymbol{R}_{f,XY}\left(\boldsymbol{\theta}_{d,XY}\right) + \sigma^2_{XY}\boldsymbol{I}_M.\end{aligned} \quad (3)$$

In (3), $\boldsymbol{I}_\kappa$ is the identity matrix of size κ, and $M = M_R M_T M_f$; the measurement noise is modeled as independent and identically distributed (i.i.d.) complex Gaussian noise with variance σ^2_{XY}. Furthermore, the DMC covariance matrix $\boldsymbol{R}_{d,XY}$ is modeled as correlated in the frequency domain ($\boldsymbol{R}_{f,XY}$). It is assumed that the DMC power delay profile follows the well-known exponential decay:

$$\psi_{XY}(\tau) = \alpha_{d,XY} e^{-\beta_{d,XY}(\tau - \tau_{d,XY})}. \quad (4)$$

In (4), $\alpha_{d,XY}$ (peak power), $\beta_{d,XY}$ and $\tau_{d,XY}$ (normalized coherence bandwidth and base delay respectively), are elements of the DMC parameter vector $\boldsymbol{\theta}_{d,XY}$ of polarization subchannel XY.

IV. Results

A. Measured Polarimetric Power Delay Profile

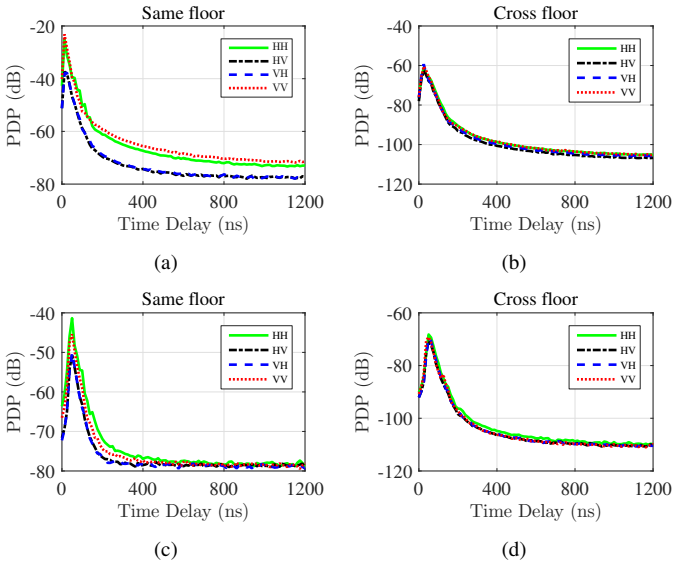

Fig. 2: PDP plots of polarimetric subchannels for "same floor", (a)-(c) and "cross floor", (b)-(d) conditions.

This section analyzes the measured power delay profile (PDP) as a function of propagation delay across four polarimetric subchannels (HH, HV, VH, and VV) for "same floor" and "cross floor" scenarios. PDPs are obtained for each polarimetric channel matrix presented in [7] and averaged over all 256 MIMO subchannels to remove small-scale fading. Fig. 2a (plot of LOS link Tx1Rx1 in Fig. 1) and Fig. 2c (plot of NLOS link Tx1Rx6 in Fig. 1), about 5 to 15 dB PDP differences were recorded between co- (HH and VV) and cross- (HV and VH) polar links. Because the transmitted waves might have undergone a small number of reflections, co-polar links are less affected (or depolarized) by those reflections compared to cross-polar links that must have been suffered from polarization mismatched before. Further, we discovered that these PDPs differences decrease as the co-polar links change from the LOS (Fig 2a) to the NLOS (Fig 2c) situations. In contrast, co-and cross-polar channels do not differ notably in the cross floor scenarios that can be seen in Fig. 2b (Tx2Rx1 link) and Fig. 2d (Tx2Rx6 link). The reason is that the radio waves reach to Rx via multiple reflections in this case, causing change of polarization states (or randomly polarized) of the waves, which leads to insignificance differences (less than 1 dB), in average, between co-and cross-polar channels. Also, the Tx2Rx1 link received nearly 10 dB more power than the Tx2Rx6 link in all polarization states, which merely represents two different locations despite both links being NLOS. These results are our contributions in this paper, which was briefly discussed in [7].

TABLE II: MEAN MEASURED XPD (dB)

	XPD_H	XPD_V
Same floor	6.9	7.5
Cross floor	1.2	0.2

B. Average Measured XPD

The purpose of this study is to quantify the cross polarization discrimination (XPD) for horizontally and vertically polarized waves for different floor levels. Each Tx-Rx link on "same floor" and "cross floor" scenarios is computed [4] as follows:

$$\text{XPD}_\text{H} = 10\log_{10}\left(\frac{\sum_p \text{PDP}_\text{HH}(\tau_p)}{\sum_p \text{PDP}_\text{HV}(\tau_p)}\right) \quad (5)$$

$$\text{XPD}_\text{V} = 10\log_{10}\left(\frac{\sum_p \text{PDP}_\text{VV}(\tau_p)}{\sum_p \text{PDP}_\text{VH}(\tau_p)}\right) \quad (6)$$

where XPD_H and XPD_V represent a horizontal and a vertical XPD respectively. τ_p is time delay at Tx-Rx link, and PDP_XY refers to PDP for both co- and cross-polar links where X and Y can be either H or V or both.

In Table II, the mean XPD (XPD_H and XPD_V) are presented for "same floor" and "cross floor" situations. Compared to the cross floor cases, XPD values of nearly 5 dB higher for horizontally and 7 dB higher for vertically polarized waves are found in the same floor cases. This indicates that the radio waves are depolarized more in the cross floor scenarios because of weak NLOS propagations; these findings are in line with the results presented in [7] for the NLOS.

C. Polarimetric Estimated SMC and DMC

In this section, we present the contributions of SMC and DMC to the total received power of polarimetric subchannels. Estimated powers of eight Tx-Rx links as a function of distances are depicted in Fig. 3. Nearly 20 dB more power is contributed by SMCs in the co-polar links (Fig. 3a and Fig. 3g) than by SMCs in the cross-polar links (Fig. 3c and Fig. 3e). Possible reason is that the higher order specular components might have undergone depolarization. This means SMC power suffered more in cross-polar links compared to co-polar links. However, DMC powers in both co-and cross-polar links do not differ significantly. The occurrence of depolarization phenomenon is further explained by the fact that

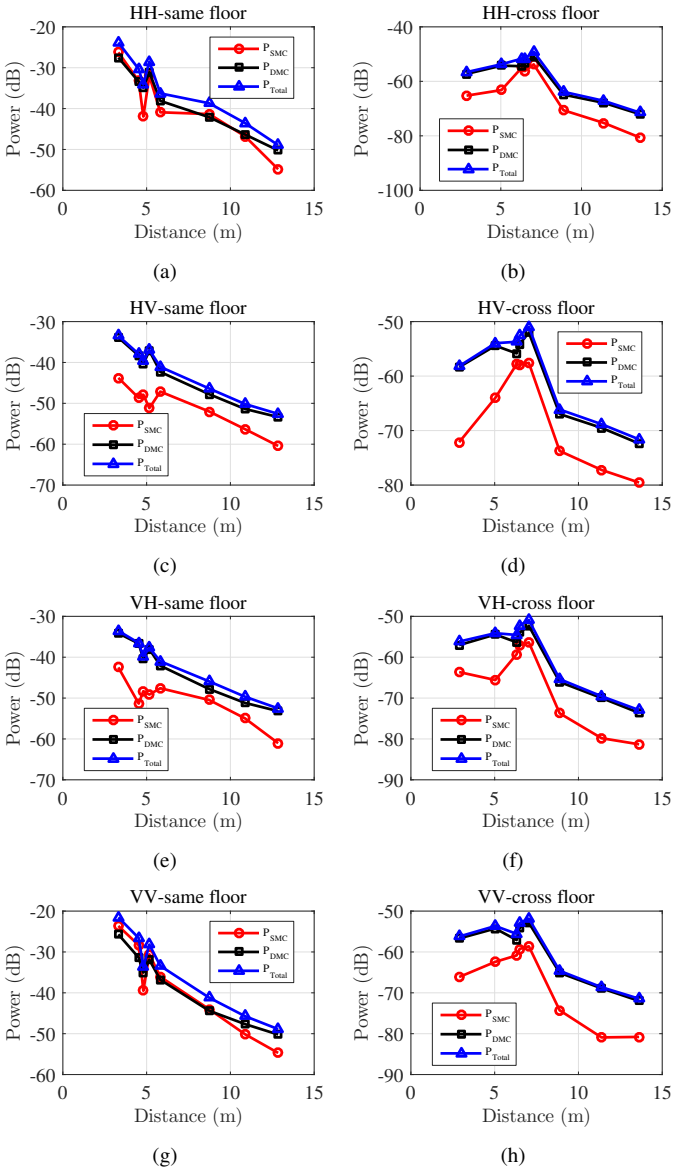

Fig. 3: Estimated powers of SMC, DMC and Total polarimetric subchannels measured across the "same floor", (a)-(c)-(e)-(g) and the "cross floor", (b)-(d)-(f)-(h) scenarios.

the contribution of DMC power in the cross floor scenarios (right column of Fig. 3) is stronger than the corresponding contribution of SMC power as it is highly probable that the specular components might be very small or acutely attenuated (similar results were reported in [7] for a large industrial scenario). A sudden increased in power near 5.2 m distance in Fig. 3 (a)-(c)-(e)-(g) refers to the LOS point. However, the increased of powers (peaks) around 6.3 m, 6.5 m, and 7 m in Fig. 3 (b)-(d)-(f)-(h) corresponds to highly scattering locations (Tx2Rx4, Tx2Tx3 and Tx2Rx5 shown in Fig. 1) where SMC paths were found to be greater than or equal to 100. These results lead us to conclude that the power does not necessarily correlate with distances significantly, specially in the cross floor scenarios, where radio waves propagate NLOS. This depends completely on Tx and Rx locations.

To complete our analysis of polarimetric indoor MIMO channels, we list the results (estimated mean, $\hat{\mu}$ and standard deviation, $\hat{\sigma}$) of the reverberation ratios in Table III for all polarimetric channels and across the "same floor" and the "cross floor" cases. The reverberation ratio is defined as the fraction of the total power contained in reverberant components (or DMCs) in [13]. We observed that the contribution of DMC power to the cross-polar channels ($\hat{\mu}$ = 83 %) is larger than the contribution of co-polar channel powers ($\hat{\mu}$ = 52 %) in both the same floor and cross floor cases. Because SMCs are stronger in the co-polar channels compared to the cross-polar channels that supposedly reduces the power of DMCs in the co-polar links. In other words, more number of multipath components are qualified for SMCs than DMCs in the co-polar links. However, co-polar channels in the cross floor scenarios contribute larger DMC power compared to the co-polar channels in the same floor scenarios (e.g, 76 % versus 58 % for HH). These results are consistent with the results that were presented in [6] [11] and higher compared to the results in [7] because the path lengths of the reflected waves might be larger for a high industrial hall in [7] compared to the small residential building, in our case, where NLOS components are stronger.

TABLE III: REVERBERATION RATIOS (%)

	HH		HV		VH		VV	
	$\hat{\mu}$	$\hat{\sigma}$	$\hat{\mu}$	$\hat{\sigma}$	$\hat{\mu}$	$\hat{\sigma}$	$\hat{\mu}$	$\hat{\sigma}$
Same floor	58.5	14.5	83.8	8.7	82.8	10.9	52.4	15.9
Cross floor	76.2	13.4	81	11	80.2	10.4	84.3	8

V. Conclusion

Analysis of PDPs, XPDs, and received power of SMC and DMC in the polarization domain is performed across the "same floor" and the "cross floor" levels for a residential building at 2.45 GHz carrier frequency. Negligible variations on four polarimetric PDPs in the "cross floor" scenarios were discovered, although some variations between co-and cross-polar channels have been reported for the "same floor" scenarios, these variations vanish as the links turn from LOS to NLOS for all four polarizations. PDP powers in the cross floor scenarios were found less than in the same floor scenarios and was also justified. Further, for the cross floor level, horizontal and vertical XPDs were respectively found 5 dB and 7 dB lower than for the same floor level. Similarly, a power difference close to 20 dB was measured for SMCs between co-and cross-polar channels in the same floor level, which was found up to 15 dB in the cross floor level. Also, we observed DMC powers were less affected in cross-polar channels compared to corresponding SMC powers, specially in same floor case. In the cross floor level, the received powers did not correlate with distances across all four polarization states. Finally, normalized contributions of DMC power (or reverberation ratio) to the total polarimetric channels were also reported and discussed.

ACKNOWLEDGMENT

The authors would like to thank Matthias Van den Bossche, M. Eng., for his help in building the channel sounding measurement system, and Jan De Beule, M. Sc. Eng., for his help during the measurements.

This research was supported by the project IUAP BESTCOM, "BElgian network on STochastic modelling, analysis, design and optimization of COMmunication systems.

REFERENCES

[1] IEEE Standards Association, "Wireless Lan Medium Access Control (MAC) and Physical Layer (PHY) Specifications," *ANSI/IEEE Std 802.11*, 1999.

[2] ZigBee Alliance, "Zigbee Specification v1.0," *ZigBee Document 053 473r00*, 2005.

[3] P. Kyritsi and C. C. Donald, "Propagation characteristics of horizontally and vertically polarized electric fileds in an indoor environment: simple model and results," *Proc. IEEE VTS 54th Veh. Technol. Conf. (VTC Fall)*, vol. 2, no. 7, pp. 1422–14 265, Mar. 2001.

[4] M. Landmann, K. Sivasondhivat, J.-I. Takada, I. Ida, and R. Thomä, "Polarization behavior of discrete multipath and diffuse scattering in urban environments at 4.5 GHz," *EURASIP J. Wireless Commun. Netw.*, vol. 1, no. 7, pp. 1–16, Jan. 2007.

[5] F. Quitin, C. Oestges, F. Horlin, and P. De Doncker, "Diffuse multipath component characterization for indoor MIMO channels," in *Proc. Eur. Conf. Antennas Propag.*, Barcelona, Spain, Apr. 2010, pp. 1–5.

[6] J. Poutanen, J. Salmi, K. Haneda, V.-M. Kolmonen, and P. Vainikainen, "Angular and Shadowing Characteristics of Dense Multipath Components in Indoor Radio Channels," *IEEE Transactions on Antennas and Propagation*, vol. 59, no. 1, pp. 1–9, 2011.

[7] D. P. Gaillot, E. Tanghe, W. Joseph, P. Laly, V.-C. Tran, M. Liénard, and L. Martens, "Polarization Properties of Specular and Dense Multipath Components in a Large Industrial Hall," *IEEE Transactions on Antennas and Propagation*, vol. 63, no. 7, pp. 3219–3228, Jul. 2015.

[8] A. Richter, "Estimation of Radio Channel Parameters: Models and Algorithms," Ph.D. dissertation, Technische Universität Ilmenau, Fakültat für Elektrotechnik und Informationstechnik, Ilmenau, DE, 2005.

[9] M. Kaske, M. Landmann, and R. Thomä, "Modelling and synthesis of dense multipath propagation components in the angular domain," *Proc. 3rd Eur. Conf. on Antennas and Propagation (EuCAP2009)*, no. 7, pp. 2641–2645, Mar. 2009.

[10] A. Richter, J. Salmi, and V. Koivunen, "Distributed Scattering in Radio Channels and its Contribution to MIMO Channel Capacity," in *European Conference on Antennas and Propagation*, Nice, FR, 2006, pp. 1–7.

[11] E. Tanghe, D. P. Gaillot, M. Liénard, L. Martens, and W. Joseph, "Experimental Analysis of Dense Multipath Components in an Industrial Environment," *IEEE Transactions on Antennas and Propagation*, vol. 62, no. 7, pp. 3797–3805, Jul. 2014.

[12] M. Landmann, M. Kaeske, R. Thoma, J.-I. Takada, and I. Ida, "Measurement Based Parametric Channel Modeling Considering Diffuse Scattering and Specular Components," in *International Symposium on Antennas and Propagation*, no. 1, 2007, pp. 153–156.

[13] G. Steinböck, T. Pedersen, and H. B. Fleury, "Distance Dependent Models for the Delay Power Spectrum of In-room Radio Channels," *IEEE Transactions on Antennas and Propagation*, vol. 61, no. 8, pp. 4327–4340, Aug. 2013.